

Prompt neutron spectrum and average neutron multiplicity in spontaneous fission of ^{252}Cf

H. Ahmadov, B. Gönül, and M. Yilmaz

Department of Engineering Physics, University of Gaziantep, 27310 Gaziantep, Turkey

(Received 13 March 2000; published 10 January 2001)

A simple analytical expression is introduced for the average neutron multiplicity depending on the fission fragment mass using directly the prompt neutron energy spectrum in the framework of statistical theory of neutron evaporation from fission fragments. The theoretical results are compared with the experimental data for the spontaneous fission of ^{252}Cf . The possibility of oscillative character of neutron average multiplicity versus fragment masses is discussed in terms of the neutron average binding energy for a given fragment mass.

DOI: 10.1103/PhysRevC.63.024603

PACS number(s): 25.85.Ca

I. INTRODUCTION

Prompt fission neutrons have become the subject of a number of detailed studies on both the fission mechanism and neutron evaporation rather than the practice for reactor calculations, in which the ^{252}Cf nucleus has been widely used due to its highly specific neutron yield.

One such study is the work of Brosa [1] on prompt neutron average multiplicity in the spontaneous fission of ^{252}Cf and ^{258}Fm involving the multimodal fission hypothesis of a fissioning nucleus and its scission at random position on the neck. In his work, Brosa developed a model for the calculation of neutron multiplicities versus fission fragment masses. Using experimental fission mode probability data and corresponding Gaussian-like mass yields of fragments, together with the neutron multiplicity estimation for a given mode, Brosa predicted a triple sawtooth behavior of average neutron multiplicities in the spontaneous fission of ^{252}Cf , which was confirmed later experimentally [2]. In describing the average neutron multiplicities against mass number, different methods such as fission fragment mass yield moments [3] and fragment average excitation energy estimation [4] were used. In a recent paper [5] the average neutron multiplicity has been calculated as a function of excitation energy involving total neutron spectrum, the fragment mass dependence has not been considered.

The purpose of this paper is to calculate the average neutron multiplicity versus fragment mass directly from the fission neutron energy spectrum. The present work shows that an analytical simple expression is available for average neutron multiplicities from which the contributions coming from free parameters in the theory used to the mass depending average neutron multiplicity can be clearly seen. We find that the average fragment excitation energy estimation, together with the neutron average binding energy, and the kinetic energy estimation mainly determine the average neutron multiplicity as has been used in a number of studies. In addition, we show that the contribution of excitation energy variance to the average neutron multiplicity and that the triple sawtooth behavior of average neutron multiplicity in the fission of ^{252}Cf can be naturally described through the present calculations.

Since our derivation of average neutron multiplicity is based on neutron energy spectrum calculations, the essence of the available calculation methods on neutron energy spec-

trum will be discussed, together with our contributions to the related formulas, in the following section. Sections III and IV present our calculation method for the prompt fission neutron spectrum in the fragment center of mass frame and average neutron multiplicities, respectively. We discuss the results in Sec. V. Concluding remarks are given in Sec. VI.

II. THEORETICAL BACKGROUND

Prompt fission neutrons have been studied experimentally and theoretically in a great number of investigations on spontaneous and induced fission of different nuclei. In these works, in general, energy and angular distributions of prompt fission neutrons in the fragment center of mass and laboratory frames, neutron average energy, multiplicity, and other characteristics of prompt neutrons have been studied. Since our calculation method of prompt neutron spectrum is nearly close to those introduced by Refs. [4,6], here we shall briefly review the works described in Refs. [4,6].

In the framework of the statistical model and in the Weisskopf representation [7], Terrell [6] calculated the fission neutron spectrum taking into account the cascade evaporation of neutrons and introducing the notion of residual excitation energy distribution. In his calculations, the compound nucleus formation cross section was assumed to be constant. The residual distribution takes into account both the initial excitation energy distribution in the Gaussian form and the cascade evaporation neutrons. Further, using the degenerate Fermi-gas model of nucleus, the residual excitation distribution is transformed to the temperature distribution of residual fragments. Carrying out numerical integrations for different temperatures, Terrell found Maxwellian forms of laboratory neutron energy spectra for the cases of ^{252}Cf spontaneous fission and neutron induced fission of ^{235}U , which were observed in the experiments.

Madland and Nix [4] introduced an analytical expression involving an exponential integral and incomplete gamma functions for the energy spectra in the fragment center of mass and laboratory systems using Terrell's representation for temperature distribution of residual fragments and constant compound nucleus cross section of neutron absorption. Comparing their calculations with experimental data on neutron induced fission of ^{235}U , they found nearly Maxwellian form in the energy region of emitted neutrons less than 5 MeV. However, it should be noted that the residual tempera-

ture (T) distribution, used in the calculations of Refs. [4,6] in the form

$$P(T)dT = \begin{cases} \frac{2T}{T_m^2} dT, & T \leq T_m \\ 0, & T > T_m \end{cases}, \quad (1)$$

where T_m is the maximum temperature that corresponds to the initial total average excitation energy \bar{U} of fission fragments being $\bar{U} = aT_m^2$ (a is the Fermi-gas level density parameter), corresponds to a constant (or regular) residual excitation energy distribution such that $P(U)dU = P(T)dT$ where U is the excitation energy and

$$P(U)dU = P(U)2aTdT = \frac{2T}{T_m^2} dT, \quad (2)$$

which yields $P(U) = 1/aT_m^2 = 1/\bar{U}$. As shown in Ref. [6], the residual distribution of excitation energy decreases with increasing excitation energy. So the linear distribution form given by Eq. (1) is somewhat incorrect, although almost the same initial average excitation energy given in Ref. [6] corresponds to both an average temperature for linear distribution ($\bar{T} = T_m$) and to a numerical integration value for more exact temperature distribution.

Further, Madland and Nix [4] carried out their calculations on compound nucleus formation cross section using different potentials within the frame of the nuclear optical model. Having an approximate calculated cross section σ_c that depends on neutron energy ε ,

$$\sigma_c = b + \frac{c}{\sqrt{\varepsilon}}, \quad (3)$$

where b and c are constant, they performed numerical integrations of neutron spectra for ^{252}Cf fission and neutron induced fission of uranium and plutonium. The comparison of their calculation results with experimental data led to a better agreement than those obtained using constant cross-section calculations.

In the same work [4], the average neutron multiplicity was calculated using

$$\bar{U} = \bar{\nu}(\bar{B}_n + \bar{\varepsilon}) + \bar{E}_\gamma \quad (4)$$

with $\bar{\nu}$, \bar{B}_n , $\bar{\varepsilon}$, and \bar{E}_γ being, respectively, the average multiplicity, average neutron binding energy, average neutron center of mass energy, and the total average prompt gamma energy.

It is noted that the theories used in Refs. [4,6] do not include fission fragment initial excitation energy variance. The approximations of shifted excitation energy distribution for the emission of cascade neutrons and residual distribution of excitation energy were not cleared out in their work, which will be explained explicitly in the present work through Sec. IV. In our calculations, we will derive an analytically simple expression for neutron energy spectrum and neutron multiplicity which depends on four terms; the fission

fragment initial excitation energy distribution parameters (most probable excitation and its variance), the neutron average binding energy, and the nuclear temperature parameter for a given fission fragment. We will compare our calculation results with the experimental data for neutron multiplicity dependence on fission fragment mass, and show that our work leads to a better agreement with the data than the work of Brosa [1].

A. Neutron evaporation spectrum formula and nuclear state density

In accordance with the principle of detailed balance [7,8], the energy distribution of neutrons emitted from compound nucleus with the excitation energy U can be written as

$$\varphi(\varepsilon, U-B) = \text{const} \times \varepsilon \sigma_c(U-B-\varepsilon, \varepsilon) \frac{\rho(U-B-\varepsilon)}{\rho(U)}, \quad (5)$$

where ε and B are the neutron kinetic and binding energies, respectively, and σ_c is a formation cross section of compound nucleus with excitation energy U . In Eq. (5), $\rho(U)$ and $\rho(U-B-\varepsilon)$ are the nuclear state densities of the initial and final states, respectively.

Considering the nucleus as a system of nucleons in the thermodynamical equilibrium state and requiring the maximality of its entropy, the energy state density of a nucleus with the excitation U may be determined by the use of the Darwin-Fowler integral method [9] reducing to

$$\rho(U) = \frac{\exp[S(U)]}{\lambda(U)}, \quad (6)$$

where $S(U)$ is the entropy and $\lambda(U)$ is the function from the second derivatives of the entropy. For the degenerate Fermi-gas model, Bethe [10] determined λ as

$$\lambda(U) \sim U^n, \quad (7)$$

where n is a fractional number. Bringing together Eqs. (5) and (6), one can write

$$\varphi(\varepsilon, U-B) = \text{const} \times \varepsilon \sigma_c(U-B-\varepsilon, \varepsilon) \frac{\exp[S(U-B-\varepsilon)]}{\lambda(U-B-\varepsilon)}. \quad (8)$$

Supposing $\varepsilon \ll U-B$, Weisskopf [8] used

$$\exp[S(U-B-\varepsilon)] \approx \text{const} \times \exp\left(-\frac{\varepsilon}{T(U-B)}\right), \quad (9)$$

where

$$T^{-1}(U-B) = \left(\frac{\partial S}{\partial U}\right)_{U=U-B} \quad (10)$$

is the thermodynamic temperature of the final nucleus with the excitation energy $(U-B)$.

In his calculations Terrell [6] used an approximation, unlike the one employed by Weisskopf, such that $|\varepsilon - \bar{\varepsilon}| \ll U$

$-B-\bar{\varepsilon}$ to determine the final state temperature from less excitation energy which differs from the corresponding Weisskopf's expression by $\bar{\varepsilon}$. However, for our calculations we shall use

$$\begin{aligned} \varphi(\varepsilon, U-B) &= \text{const} \times \varepsilon \sigma_c(U-B-\varepsilon, \varepsilon) \\ &\times \frac{\exp[-\varepsilon/T(U-B)]}{\lambda(U-B-\varepsilon)}, \end{aligned} \quad (11)$$

which can be obtained by the substitution of Eq. (9) into Eq. (8).

A more contemporary model [5], the so-called ‘‘phenomenological version of the generalized superfluid model of nuclear level density,’’ gives no new information regarding the description of the prompt fission neutron spectrum.

B. Compound nucleus formation cross section

Obviously, the abundance of data to which one is accustomed from work with stable nuclei certainly cannot be expected for fission fragments which are neutron enriched nuclei with high excitation energies. Hence the existing experimental information regarding the stable nuclei is usually extrapolated to gather some information for the compound nucleus formation cross sections. Another way is to calculate compound nucleus formation cross section for different neutron energies for a mass considered theoretically.

Experimental data for σ_c shows $1/\sqrt{\varepsilon}$ behavior for the incident neutron energy range starting from thermal energy to ~ 1 MeV. For the higher energies the cross section is almost constant. Calculations [4], including the compound nucleus formation cross section expressed in Eq. (3), where the constants a and b are based on the optical model involving different potentials, justify this behavior.

C. Neutron evaporation spectrum from fission fragments

As discussed in Sec. II A, Weisskopf [7] used an exponential expression, Eq. (9), in describing level density of compound nucleus for the case $\varepsilon \ll (U-B)$. Stavinsky [11], to describe the average properties of a nuclear system within the Hibbs canonical assembly, proposed a fixed excitation for nuclei due to the isolation but assumed the thermodynamical fluctuation of the temperature around an average temperature value, \bar{T} . Using the Gaussian distribution of temperature and supposing the relation

$$U = a\bar{T}^2 \quad (12)$$

between nuclear excitation and average temperature, he proved that the relation given by Weisskopf, Eq. (9), is not only valid for the condition $\varepsilon \ll U-B$ but for the whole range of ε , namely $0 \leq \varepsilon \leq U-B$, replacing T in Eqs. (9) and (11) with \bar{T} .

Here we note that the thermodynamical temperature of a nucleus given by Eq. (10), which also appears in Eq. (11), differs from the nuclear temperature (T'), which is determined through

$$\begin{aligned} \frac{1}{T'} &= \frac{d}{d(U-B-\varepsilon)} \ln \frac{\varphi(\varepsilon, U-B)}{\varepsilon \sigma_c(U-B-\varepsilon, \varepsilon)} \\ &= \frac{d}{d(U-B-\varepsilon)} \ln \rho(U-B-\varepsilon) \\ &= -\frac{d}{d\varepsilon} \ln \rho(U-B-\varepsilon). \end{aligned} \quad (13)$$

In practice, T' is determined in measuring the neutron evaporation spectra from the reactions (n, n') and (p, n) at different incident energies, which correspond to different nuclear excitations, and making assumptions regarding the behavior of $\sigma_c(U-B-\varepsilon, \varepsilon)$ on U and ε . In this case $\varphi(\varepsilon, U-B)$ represents the neutron spectrum either for (n, n') or for (p, n) reactions. To describe the nuclear level density, a variety of models have been used, including the degenerate Fermi-gas model, the Fermi-gas model with the residual interaction in the form of pairing energy, the superfluid model of nuclear matter, and the so-called generalized superfluid model [12,13]. In the superfluid model, the energy of the transition of the nuclear matter to the superfluid state is close to the neutron binding energy. However, in investigating prompt fission neutron spectra, fragment excitations are considered at high excitations until 35–40 MeV, starting from the neutron binding energy. In such region of nuclear excitation energy, the superfluid model is reduced to the degenerate Fermi-gas model with the renormalization of the excitation energy to the lower value shifting by a condensation energy. One of the main parameters of this model, the nuclear level density parameter a that relates to the thermodynamical temperature with excitation energy, and which depends on nuclear shell structure, can be determined most reliably from the neutron resonance data of compound nucleus at the excitations near the neutron binding energy. But neutron resonance data are insufficient in describing the nuclear level density dependent on excitation energy. Alternative methods are the use of (n, n') and (p, n) reactions where neutrons are assumed as evaporating from the compound nucleus. Having used neutron spectrum measurements from the neutron inelastic scattering and from (p, n) reactions, one can verify fulfillment of Eq. (12) or one can determine the nuclear temperature through Eq. (13) in a wide region of nuclear excitations. Some results of such studies are described in Refs. [14–16]. In these works, almost constant nuclear temperatures were obtained for different nuclei in a wide region of the given nuclear excitations when emission of a few neutrons is energetically possible, and in some cases the constant temperature approximation gave a better description of nuclear state density than that of the Fermi-gas model at excitation energies higher than neutron binding energy. In addition, such description has a more general character which is not limited to the magic or near magic nuclei.

Thus, the approximate constancy of a nuclear temperature in describing the nuclear level density of a nucleus in a wide region of the excitation energies makes it possible to use this result in the application for the prompt fission neutron energy spectrum calculations. In this case the thermodynamical temperature in Eq. (11) may be admitted as a nuclear tempera-

ture. Assuming $\sigma_c(U-B-\varepsilon, \varepsilon)$ as constant due to qualitative weighting of our calculations, for the energy spectrum of neutrons emitted from fragment with excitation U , we write

$$\varphi(\varepsilon, U-B) = \frac{\varepsilon \exp(-\varepsilon/T)}{T^2 F[(U-B)/T]}, \quad (14)$$

where the appearance of the function $F[(U-B)/T]$, which is in the form

$$F[(U-B)/T] = 1 - [1 + (U-B)/T] \exp[-(U-B)/T], \quad (15)$$

is due to the normalization condition

$$\int_0^{U-B} \varphi(\varepsilon, U-B) d\varepsilon = 1. \quad (16)$$

The neutron evaporation energy spectrum in the fragment center of mass system in the form of Eq. (14) is to be considered as isotropic and emitted from fully accelerated fragments in accordance with the observations of Ref. [4]. We will assume different nuclear temperature parameters for different initial fission fragments. The competition between γ and neutron emissions is neglected due to low angular momentum fission fragment considerations [17].

D. Initial excitation energy distribution of fission fragments

Experimental investigations do not provide any information on the initial excitation energy distribution of single fission fragments, but do yield information regarding the total kinetic energy distribution of two complementary fragments. Knowledge on single fragment excitation distribution can be derived either from data involving total kinetic energy distribution making a supposition on energy transmission between complementary fragments or from data on neutron number distribution [6]. Experimental total kinetic energy distribution of fission fragments is approximated to the normalized Gauss distribution,

$$P(E) = \frac{1}{\sqrt{2\pi\sigma}} \exp\left[-\frac{(E-E_0)^2}{2\sigma^2}\right], \quad (17)$$

where E and E_0 are the total kinetic energy and most probable total kinetic energy, respectively, and σ is the variance of total kinetic energy. Using the expression for Q , which is the energy release in fission, in terms of E and total excitation energy U for the given mass numbers A_1 and A_2 as

$$Q(A_1, A_2) = E(A_1, A_2) + U(A_1, A_2), \quad (18)$$

one can find for the total excitation energy distribution in the form

$$P(U) = \frac{1}{\sqrt{2\pi\sigma}} \exp\left[-\frac{(U-U_0)^2}{2\sigma^2}\right], \quad (19)$$

where U_0 is the most probable total excitation energy. If we suppose that independent excitation energy distributions of fragments are in Gaussian form then the total distribution of $U = U_1 + U_2$ is given as

$$\begin{aligned} P(U) &= \int_{-\infty}^{\infty} P(U_1)P(U_2)dU_1 \\ &= \int_{-\infty}^{\infty} P(U_1)P(U-U_1)dU_1 \\ &= \frac{1}{\sqrt{2\pi\sigma}} \exp\left[-\frac{(U-U_0)^2}{2\sigma^2}\right]. \end{aligned} \quad (20)$$

Here $P(U_1)$ and $P(U_2)$ are normalized Gauss distributions for complementary fragments and $U_0 = U_{10} + U_{20}$, $\sigma^2 = \sigma_1^2 + \sigma_2^2$, where U_{10} , σ_1 and U_{20} , σ_2 are corresponding excitation energies and variances of fragments, respectively.

However, the physically acceptable values of excitation energies of fragments lie between $0 \leq U_1 \leq U$, $0 \leq U_2 \leq U$, so that Eq. (20) becomes

$$P(U) = \int_0^U P(U_1)P(U_2)dU_1. \quad (21)$$

It seems impossible to obtain a simple form in Eq. (21) for the free values of distribution parameters. Supposing $U_{10} = U_{20} = U_0/2$ and $\sigma_1 = \sigma_2 = \sigma/\sqrt{2}$, Eq. (21) reduces to the form

$$P(U) = \frac{1}{\sqrt{2\pi\sigma}} \operatorname{erf}\left(\frac{U}{\sqrt{2}\sigma}\right) \exp\left[-\frac{(U-U_0)^2}{2\sigma^2}\right], \quad (22)$$

where

$$\operatorname{erf}\left(\frac{U}{\sqrt{2}\sigma}\right) = \frac{2}{\sqrt{\pi}} \int_0^{U/\sqrt{2}\sigma} \exp(-t^2) dt. \quad (23)$$

Differences between the numerical results obtained by Eqs. (20) and (22) get larger if $U/\sqrt{2}\sigma < 1$, whereas the results of both equations approach each other when $U/\sqrt{2}\sigma > 1$. Thus, in the present calculations the distribution function in Eq. (22) is not used due to its nonobservable behavior.

More general forms of excitation energy distributions of two complementary fragments may be given by a two-dimensional normal distribution with the correlation, which is characterized by the coefficient of correlation ρ_{12} , between excitation energies of fragments. In this case, each fragment excitation distribution is expressed through the conditional distribution when the total excitation energy is given. Due to the experimental indication [18] that the coefficient ρ_{12} approaches -0.1 for the fragments in the spontaneous fission of ^{252}Cf , which means the use of Eq. (20) is appropriate for the single fragment initial excitation energy distribution calculations presented in this letter involving Gauss distribution function normalized as

$$\int_B^\infty P(U)dU=1, \quad (24)$$

where B is the neutron binding energy. Hence, the distribution function used in the present calculations takes the form

$$P(U)=\frac{2}{\sqrt{2\pi}\varphi}\frac{\exp[-(U-U_0)^2/2\sigma^2]}{1+\Phi[(U_0-B)/\sigma]}, \quad (25)$$

where

$$\Phi[(U_0-B)/\sigma]=\frac{2}{\sqrt{2\pi}}\int_0^{(U_0-B)/\sigma}\exp(-t^2/2)dt \quad (26)$$

with U_0 and σ being the most probable excitation energy and excitation variance of the single fission fragment, respectively.

E. Isobaric charge distribution of fission fragments and neutron binding energy

Bowman *et al.* [19] extracted average neutron binding energies from their experiment on prompt fission neutrons of ^{252}Cf spontaneous fission, which correspond to the most probable charge Z_p that gives the maximum energy release for a given pair of fission fragments. In a number of experimental works [20–23] the charge distribution of fission fragments in the spontaneous fission of ^{252}Cf was studied for the final product, in which the charge distribution is represented by the Gauss function having most probably charge Z_p and charge variance σ_Z . Then the final product mass is transformed to the primary (pre-neutron emission) mass [21,22]. As has been shown in Ref. [22], the charge polarization parameter $\Delta Z=Z_p-Z_{\text{UCD}}$, where Z_{UCD} is a charge value in the unchanged charge density distribution hypothesis [$Z_{\text{UCD}}=(Z_{\text{fis}}/A_{\text{fis}})A$, where Z_{fis} and A_{fis} are charge and mass numbers of fissioning nucleus, respectively, A is a primary fragment mass] does not exceed a value of -0.5 for different primary fission fragment masses in the spontaneous fission of ^{252}Cf . The relation

$$Z_p(h)=Z_p(\text{UCD})-0.37, \quad Z_p(l)=Z_p(\text{UCD})+0.37 \quad (27)$$

obtained by Erten and Aras in Ref. [21] for all the heavy and light mass regions in the spontaneous fission of ^{252}Cf are used in our present calculations. In our estimation of neutron average binding energies we make use of mass tables of Garvey *et al.* [23].

III. PROMPT NEUTRON ENERGY SPECTRUM CALCULATION IN THE FRAGMENT CENTER OF MASS FRAME

The first emitted neutron energy spectrum expression used in our calculations is given as

$$N_1(\varepsilon)=\int_{B_1+\varepsilon}^\infty P(U)\varphi(\varepsilon,U-B_1)dU, \quad (28)$$

where B_1 is the binding energy of the first emitted neutron. The terms $P(U)$ and $\varphi(\varepsilon,U-B_1)$ in Eq. (28) have been discussed in Secs. IIC and IID. It is clear that

$$\int_0^\infty N_1(\varepsilon)d\varepsilon=1. \quad (29)$$

Thus, the ν th ($\nu \geq 2$) emitted neutron energy spectrum expression is

$$\begin{aligned} N_\nu(\varepsilon) &= \int_{\sum_{i=1}^\nu B_i+\varepsilon}^\infty P(U)dU \int_0^{U-\sum_{i=1}^\nu B_i} d\varepsilon_1 \varphi(\varepsilon_1, U-B_1) \cdots \\ &\times \int_0^{U-\sum_{i=1}^\nu B_i-\sum_{i=1}^{\nu-2} \varepsilon_i-\varepsilon} d\varepsilon_{\nu-1} \\ &\times \varphi\left(\varepsilon_{\nu-1}, U-\sum_{i=1}^{\nu-1} B_i-\sum_{i=1}^{\nu-2} \varepsilon_i\right) \\ &\times \varphi\left(\varepsilon, U-\sum_{i=1}^\nu B_i-\sum_{i=1}^{\nu-1} \varepsilon_i\right). \end{aligned} \quad (30)$$

Here ε_i and B_i are kinetic and binding energies of the i th neutron, respectively.

The energy spectrum of all neutrons is determined as

$$N(\varepsilon)=\sum_{i=1}^\nu N_i(\varepsilon). \quad (31)$$

Clearly Eq. (31) is normalized to the average number of neutrons such that

$$\int_0^\infty N(\varepsilon)d\varepsilon=\bar{\nu}. \quad (32)$$

For simplicity, Eq. (30) can be transformed to the form

$$\begin{aligned} N_\nu(\varepsilon) &= \int_0^\infty d\varepsilon_1 \cdots \int_0^\infty d\varepsilon_{\nu-1} \\ &\times \int_{\sum_{i=1}^\nu B_i+\sum_{i=1}^{\nu-1} \varepsilon_i+\varepsilon}^\infty P(U)\varphi(\varepsilon_1, U-B_1) \cdots \\ &\times \varphi\left(\varepsilon, U-\sum_{i=1}^\nu B_i-\sum_{i=1}^{\nu-1} \varepsilon_i\right) dU. \end{aligned} \quad (33)$$

As the function F determined by Eq. (15) $F[(U-\sum_{i=1}^\nu B_i-\sum_{i=1}^{\nu-1} \varepsilon_i)/T] \cong 1$, for each $\nu \leq \nu-1$, and introducing a new variable $U-\sum_{i=1}^\nu B_i-\sum_{i=1}^{\nu-1} \varepsilon_i \equiv Z$ one can reduce Eq. (33) to the form

$$\begin{aligned} N_\nu(\varepsilon) &= f(\varepsilon) \int_0^\infty d\varepsilon_1 f(\varepsilon_1) \cdots \times \int_0^\infty d\varepsilon_{\nu-1} f(\varepsilon_{\nu-1}) \\ &\times \int_0^\infty \left[\frac{P(Z+\sum_{i=1}^\nu B_i+\sum_{i=1}^{\nu-1} \varepsilon_i)}{F(Z/T)} \right] dZ, \end{aligned} \quad (34)$$

where $f(\varepsilon_i) \equiv \varepsilon_i/T^2 \exp(-\varepsilon_i/T)$. To work out Eq. (34) we need to introduce an average binding energy \bar{B} of a given cascade as $\sum_{i=1}^{\nu} B_i = \nu\bar{B}$. Then we have

$$\begin{aligned}
N_{\nu}(\varepsilon) &= f(\varepsilon) \int_{\varepsilon}^{\infty} \frac{dZ}{F(Z/T)} \int_0^{\infty} X_1 dX_1 \cdots \\
&\times \int_0^{\infty} X_{\nu-1} dX_{\nu-1} P \left[\left(\frac{Z}{T} + \frac{\nu\bar{B}}{T} + \sum_{i=1}^{\nu-1} X_i \right) T \right] \\
&\times \exp \left(- \sum_{i=1}^{\nu-1} X_i \right), \quad (35)
\end{aligned}$$

where $X_i \equiv \varepsilon_i/T$. Further, integrating Eq. (35) as in Ref. [24] we obtain

$$\begin{aligned}
N_{\nu}(\varepsilon) &= \frac{f(\varepsilon)}{\Gamma[2(\nu-1)]} \int_{\varepsilon}^{\infty} \frac{dZ}{F(Z/T)} \times \int_0^{\infty} X^{2(\nu-1)-1} \\
&\times P \left[\left(\frac{Z}{T} + \frac{\nu\bar{B}}{T} + X \right) T \right] \exp(-X) dX. \quad (36)
\end{aligned}$$

Here $\Gamma[2(\nu-1)] = [2(\nu-1)-1]!$. The above expression is applicable for $\nu \geq 2$. The first neutron spectrum given by Eq. (28) takes the form in terms of new variables

$$N_1(\varepsilon) = f(\varepsilon) \int_{\varepsilon}^{\infty} \frac{P[(Z/T + \bar{B}/T)T]}{F(Z/T)} dZ. \quad (37)$$

To make clear the validity of Terrell's approximation of shifted excitation energy distribution for evaporation of neutrons other than the first one we need to replace the gamma distribution $\Gamma(X) = \{1/\Gamma[2(\nu-1)]\} X^{2(\nu-1)-1} \exp(-X)$ in Eq. (36) by the Dirac delta function, then

$$\frac{1}{\Gamma[2(\nu-1)]} \int_0^{\infty} X^{2(\nu-1)-1} P(Z + \nu\bar{B} + XT) \exp(-X) dX \cong 1. \quad (38)$$

Therefore, Eq. (36) becomes

$$N_{\nu}(\varepsilon) = f(\varepsilon) \int_{\varepsilon}^{\infty} \frac{dZ}{F(Z/T)} P[Z + \nu\bar{B} + 2(\nu-1)T]. \quad (39)$$

Comparing Eq. (39) with Eq. (37) we come to the conclusion that the excitation energy distribution for the ν th emitted neutron is derived from the initial distribution shifted by a quantity $(\nu-1)(\bar{B} + 2T)$ which corresponds to an average excitation energy carried away by $\nu-1$ neutrons emitted from fragment. Thus, the validity of Terrell's approximation [6] depends upon Eq. (38). Expanding the left-hand side of Eq. (38) using the saddle point method it can be easily shown that Eq. (38) is valid if $T/\sigma \ll 1$ or if $\sigma > 2T(\nu-1)$ for $\nu \geq 2$, where σ comes from the definition of P given by Eq. (25).

To proceed, the sum given by Eq. (31) is replaced by an integral, see Ref. [25], for the cases $\bar{B} > 4T$ and $\sigma \gg T$. The resulting expression for the total energy spectrum is then

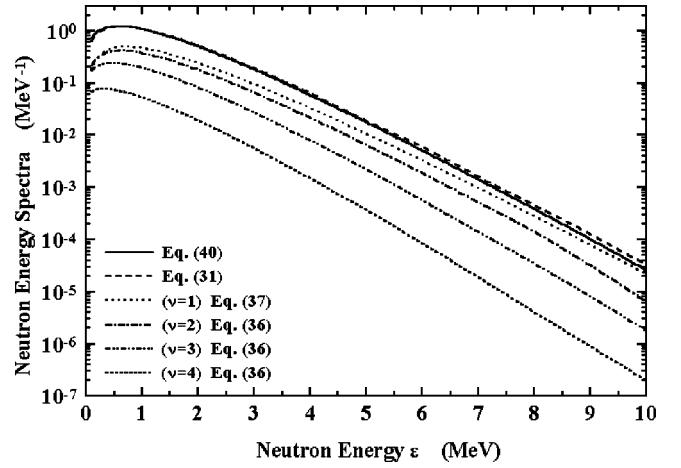


FIG. 1. Comparison of the energy spectrum $N(\varepsilon)$ obtained by Eq. (40) with those calculated by the discrete sum of Eq. (31) for the fragment $Z=43$, $A=110$ (with four significant terms).

$$\begin{aligned}
N(\varepsilon) &= \frac{\varepsilon \exp(-\varepsilon/T)}{\bar{B}T^2 \{1 + \Phi[(U_0 - \bar{B})/\sigma]\}} \\
&\times \int_{\varepsilon}^{\infty} \frac{dZ}{F(Z/T)} \int_{(Z-\alpha)/\sigma}^{\infty} \frac{2dt}{\sqrt{2\pi}} \exp\left(-\frac{t^2}{2}\right), \quad (40)
\end{aligned}$$

where $\alpha = U_0 - \bar{B}$.

To show the quality of the approximation in Eq. (40) we illustrate in Fig. 1 the comparison of the energy spectrum $N(\varepsilon)$ obtained by Eq. (40) with those calculated by the discrete sum of Eq. (31) for the fragment $Z=43$, $A=110$ (with four significant terms). The results are found in agreement.

The external integral in Eq. (40) is the corresponding analytical form of, which is more exact than, the numerical residual distribution of excitation energy introduced by Terrell [6]. The function F in Eq. (40), whose explicit form has been given by Eq. (15), may be approximated as

$$F^{-1}(X) \approx 1 + \frac{2}{X^2} \quad (41)$$

and the expression for the total neutron energy spectrum in fragment center of mass system, Eq. (40), can be worked out numerically. Comparison of calculated neutron energy spectrum with the experimental data given by Ref. [19] yielded good agreement [25].

Equation (40) used in our calculations involves initial parameters of theory, such as the most probable excitation energy U_0 and the excitation variance σ . However, we cannot directly determine these parameters either from data or from the theory for a single fragment. Hence we use the assumptions discussed in the following for the physically acceptable values of these parameters.

As has been discussed in Sec. II D, there is a relationship between the parameters of complementary fragments A_1 and A_2 such as

$$\begin{aligned}
\sigma_1^2 + \sigma_2^2 &= \sigma^2, \\
U_{10} + U_{20} &= U_0 \quad (42)
\end{aligned}$$

in which U_{10} , U_{20} are determined from experimental data on average number of neutrons for a given fragment mass. One can identify the most probable fragment excitation energy $U_{i0}(A_i)$, $i = 1, 2$, to the average fragment excitation $\bar{U}(A_i)$ as follows:

$$U_{i0}(A_i) \equiv \bar{U}(A_i) = \bar{\nu}(A_i) [\bar{B}(A_i) + \bar{\epsilon}(A_i)] + \bar{E}_\gamma(A_i), \quad (43)$$

where $\bar{\nu}$ is the average neutron number. In Eq. (43), $\bar{B}(A)$, $\bar{\epsilon}(A)$, and $\bar{E}_\gamma(A)$ are the neutron average binding energy, neutron average energy, and average gamma energies, respectively, for the corresponding fragment. It is worth noting that, really, the value of $\bar{U}(A_i)$ must be somewhat greater than the value of $U_{i0}(A_i)$ due to the condition given in Eq. (24). Unlike the case of excitation energies, we cannot write a simple expression similar to Eq. (43) for the single fragment excitation variance. Here we use $\sigma_1 = \sigma(A_1)$, $\sigma_2 = \sigma(A_2)$, and $\sigma \equiv \sigma(A_1, A_2)$ for complementary fragment excitation variances and total excitation energy variance, respectively. From Eq. (42) and supposing $\sigma(A_1) = \sigma(A_2)$ we arrive at

$$\sigma(A_1) = \sigma(A_2) = \frac{\sigma(A_1, A_2)}{\sqrt{2}}. \quad (44)$$

Clearly one can use Eqs. (43) and (44) in estimating the parameters and to calculate the total energy spectrum by Eq. (40) in the center of mass frame.

Transformation of the neutron energy spectrum from the center of mass frame to the laboratory system is necessary for the comparison of theoretical calculations of angular distribution and of energy distribution of prompt neutrons with the corresponding experimental data. Experimental investigation in Ref. [2], together with a number of other experiments, confirmed the suppositions that prompt fission neutrons are emitted only from fully accelerated fragments, and the emission is isotropic in the fragment center of mass system. Application of Eq. (40) to the spontaneous fission of ^{252}Cf in describing the angular distribution of prompt neutrons resulted in the reproduction of data in good agreement [26]. In Sec. IV we will discuss the calculation method used in the present work for the prompt neutron multiplicity in light of the discussion given here.

IV. PROMPT NEUTRON MULTIPLICITY CALCULATION

Provided $\sigma/T \gg 1$ one can easily find from Eqs. (32) and (36) the following analytical expression for the neutron multiplicity:

$$\bar{\nu} = \sum_{\nu=1}^{\infty} \frac{\exp[2(\nu-1)^2 T^2 / \sigma^2]}{[1 + \Phi(\alpha/\sigma)]} \times \left\{ 1 + \Phi \left[\frac{\alpha - (\nu-1)(\bar{B} + 2T)}{\sigma} \right] \right\}. \quad (45)$$

The above-mentioned series converges according to D'Alambert's rule, which provides us to replace the sum in Eq. (45) with its integral form. Further, using the method of saddle point for the parameters $\alpha \sim \sigma \sim \bar{B}$, Eq. (45) is transformed to

$$\bar{\nu} = \frac{1}{\bar{B} + 2T} \times \left[\alpha \frac{\sqrt{2\pi}}{2} + \sigma \frac{\exp(-\alpha^2/2\sigma^2)}{1 + \Phi(\alpha/\sigma)} \right], \quad (46)$$

which can be rearranged as

$$\begin{aligned} \bar{\nu} &= \sqrt{\frac{\pi}{2}} \frac{\sigma}{\bar{B} + 2T} \times \left[\delta + \sqrt{\frac{2}{\pi}} \frac{\exp(-\delta^2/2)}{1 + \Phi(\delta)} \right] \\ &= \sqrt{\frac{\pi}{2}} \frac{\sigma}{\bar{B} + 2T} \times f(\delta), \end{aligned} \quad (47)$$

where $\delta \equiv \alpha/\sigma$ and

$$f(\delta) \equiv \left[\delta + \sqrt{\frac{2}{\pi}} \frac{\exp(-\delta^2/2)}{1 + \Phi(\delta)} \right]. \quad (48)$$

In sum, a simple analytical expression has been found for the neutron average number which depends on parameters σ , \bar{B} , T , and $\alpha (= \bar{U} - \bar{B})$. To the best of our knowledge the result given by Eq. (47) is original, because it has been obtained directly from the neutron energy spectrum for a given fission fragment and it involves all the initial parameters of the theory used explicitly through the clear simple expression. In addition, to compare our theoretical results obtained by Eq. (47) with the related data, Eq. (47) should be written in the explicit form, considering $\bar{\nu} \equiv \bar{\nu}^{\text{th}}(A)$, $\sigma \equiv \sigma(A)$, $\bar{B} \equiv \bar{B}(A)$, $T \equiv \bar{T}(A)$, and $\delta \equiv \delta(A)$,

$$\bar{\nu}^{\text{th}}(A) = \sqrt{\frac{\pi}{2}} \frac{\sigma(A)}{\bar{B}(A) + 2\bar{T}(A)} f[\delta(A)]. \quad (49)$$

The denominator of the term $\sigma(A)/[\bar{B}(A) + 2\bar{T}(A)]$ in Eq. (49) represents an average energy carried out by an emitted neutron and the numerator denotes an initial excitation energy variance, which makes the whole expression physically meaningful due to the direct proportionality of $\bar{\nu}(A)$ to this term. The term $f[\delta(A)]$ in Eq. (49) has a linear behavior for the values of $\delta \leq 2$, because the exponential function in Eq. (48) vanishes in this region, whereas for the domain of $\delta \geq 1.5$ $f[\delta(A)]$ takes contribution from the average excitation energy involved in δ and from the initial excitation energy distribution function appearing in the second term of Eq. (48). This is demonstrated in Fig. 2. It is worth noting that for the case of $\delta \geq 2$, Eq. (49) becomes

$$\bar{\nu}^{\text{th}}(A) = \sqrt{\frac{\pi}{2}} \frac{\alpha}{\bar{B}(A) + 2\bar{T}(A)}, \quad (50)$$

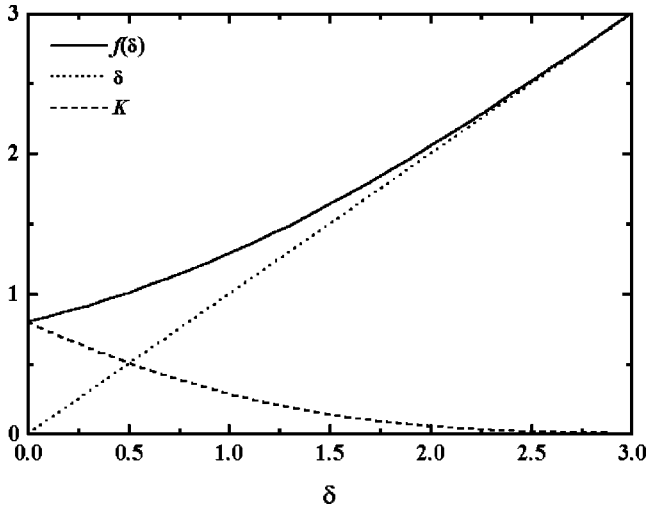


FIG. 2. Behavior of the function $f(\delta)$ (solid line) given by Eq. (48) and its components δ (dotted line) and $K \equiv [\sqrt{2/\pi}] \exp(-\delta^2/2)/[1 + \Phi(\delta)]$ (dashed line) vs δ .

which differs by a factor of $\sqrt{\pi/2}$ than the usually used, e.g., Ref. [4], form of the average neutron multiplicity.

In estimating the values of the parameters used— α , σ , and δ —we use the related data of Ref. [2] and the mass table on neutron binding energies given by Ref. [23]. For the estimation of $\bar{T}(A)$ and $\bar{E}_\gamma(A)$ we consider the relations $\bar{\epsilon}(A) = 2\bar{T}(A)$ and $\bar{E}_\gamma(A) = \bar{B}(A)/2$.

V. RESULTS AND DISCUSSION

From Eq. (49) it is obvious that the average binding energy values considerably affect the average neutron multiplicity calculations. This puts forward the significance of using a powerful method to determine reliable average binding energies for a given fragment mass. For clarification, in Fig. 3 we present our calculation results obtained by the use of

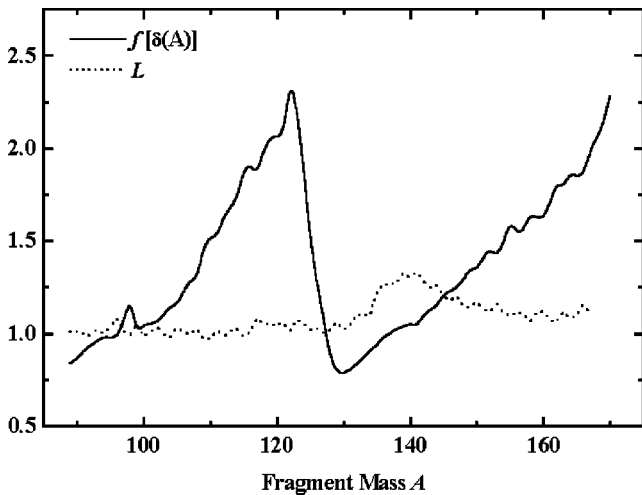


FIG. 3. Behavior of $f[\delta(A)]$ (solid line) and $L \equiv \sigma(A)/[B(A) + 2\bar{T}(A)]$ (dotted line) vs the fragment mass. Neutron average binding energies are taken from Ref. [19].

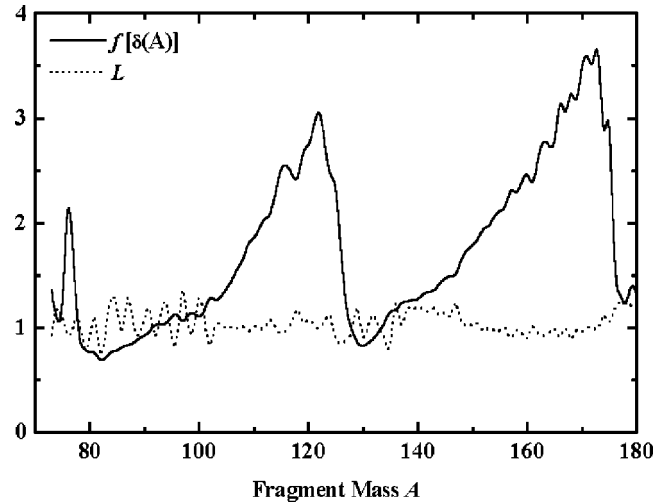


FIG. 4. The same as for Fig. 3, but neutron average binding energies are estimated by the use of Eq. (27) and of the mass table in Ref. [23].

binding energy values taken from Ref. [19] for the factors $\sigma(A)/[\bar{B}(A) + 2\bar{T}(A)]$ and $f[\delta(A)]$ appearing in Eq. (49), while Fig. 4 illustrates the results obtained through the use of average binding energy predictions calculated from the most probable charges by Eq. (27). The other parameters used in both calculations are the same and are taken from Ref. [2]. The main contribution to average neutron multiplicity calculation comes from the term $f[\delta(A)]$. It is clear from Fig. 4 that the ratios $\sigma(A)/[\bar{B}(A) + 2\bar{T}(A)]$ and $f[\delta(A)]$ oscillate with respect to A values due to neutron average binding energies. The present neutron multiplicity calculation results are compared with the data of Ref. [2] in Figs. 5 and 6. In Fig. 5, for comparison reasons, the fragment masses are limited to the interval in between 87 and 167 due to the compared average neutron binding energy estimations of

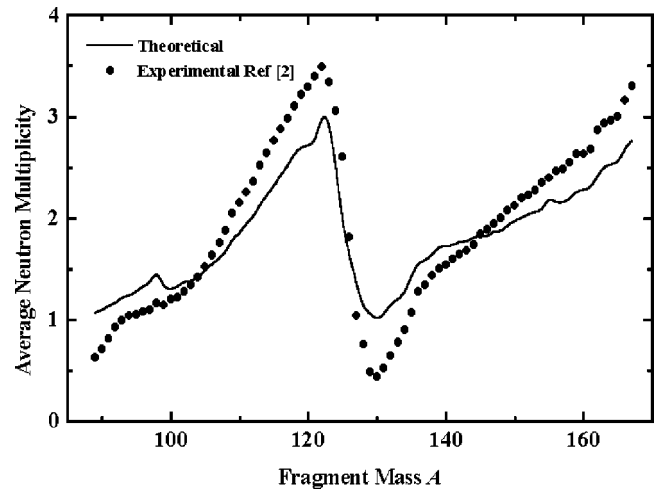


FIG. 5. The average neutron multiplicity vs the fragment mass. Solid line is the calculation result obtained by Eq. (49). Neutron average binding energies are taken from Ref. [19]. The experimental data of Ref. [2] are represented by the closed circles.

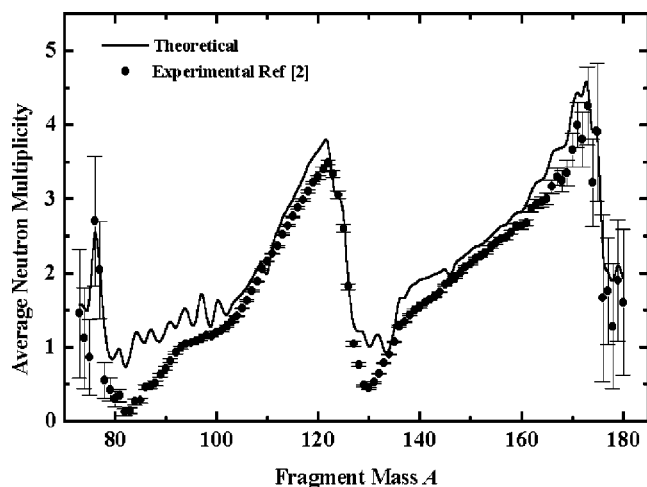


FIG. 6. The same as for Fig. 5, but neutron average binding energies are estimated by the use of Eq. (27) and of the mass table in Ref. [23].

Ref. [19]. The average neutron energy data of interest in Ref. [2] were given in the same interval. However, the average neutron energy data of Ref. [2] are extrapolated to a wide range of fragment masses in Fig. 6 to provide insight into the reliability of our neutron multiplicity calculations. The quantitative coincidence between the theory and data takes place in the wide region of masses except the regions around $A = 130$ and $A = 80-90$, where δ has values which make it unfeasible using the approximation given by Eq. (46). The triple sawtooth behavior appears explicitly in our calculation results.

In Fig. 7, the contribution of the exponential part in Eq. (48) to the average neutron multiplicity calculations is demonstrated. The comparison of calculated average neutron multiplicities (solid line) obtained by Eq. (49) with another calculation result (dotted line) obtained by Eq. (50) makes it clear that in the mass regions around $A = 130$ and $A = 80-90$ the contribution of the exponential part is considerably large. Apparently, a more exact estimation of Eq. (45) may reproduce data with a better agreement. The present calculation results also require improvement of the experimental data.

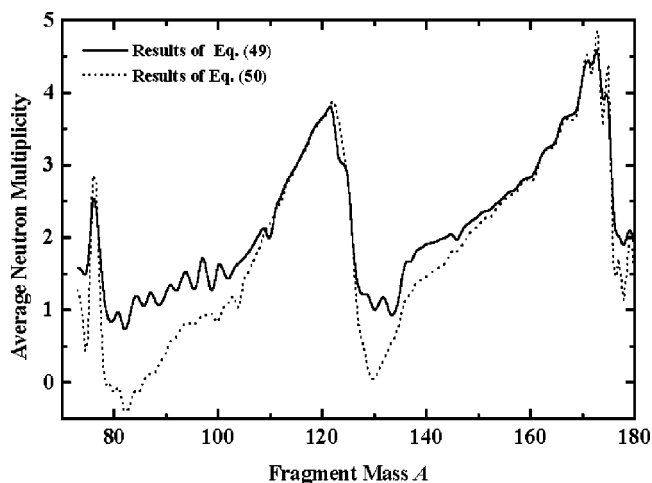


FIG. 7. Contribution of the exponential part of Eq. (48) to the average neutron multiplicity. The solid line is the calculation result of Eq. (49). The dotted line is the calculation result obtained by Eq. (50).

VI. CONCLUSION

In this work, a mathematically simple and novel expression for the calculation of average neutron multiplicity versus fragment masses has been introduced. This analytical expression involves the initial parameters of the model used, such as the most probable initial excitation energy and its variance, average neutron binding energy and nuclear temperature which has been considered constant in our calculations for the neutron cascade of the given primary fragment. A more frequently used expression that is similar to Eq. (50) for average neutron multiplicity calculations appears as a dominated term in the general expression developed, Eq. (49), which leads to a better description of the data. The oscillations seen, in particular in the fragment mass regions around $80-100$ and from 130 to 140 in the present calculations, are due to the perturbations in the values of the average neutron binding energies.

ACKNOWLEDGMENTS

One of the authors (H.A.) is grateful to Dr. F.-J. Hamsch for providing the numerical data on total kinetic energy distribution and its variance, and on the average neutron multiplicity, in spontaneous fission of ^{252}Cf .

- [1] U. Brosa, Phys. Rev. C **38**, 1944 (1988).
 [2] C. Budtz-Jorgensen and H.-H. Knitter, Nucl. Phys. **A490**, 307 (1988).
 [3] J. Terrell, Phys. Rev. **127**, 880 (1962).
 [4] David G. Madland and J. R. Nix, Nucl. Sci. Eng. **81**, 213 (1982).
 [5] M. I. Svirin, G. N. Smirenkin, and F. J. Hamsch, Phys. At. Nucl. **59**, 923 (1996).
 [6] J. Terrell, Phys. Rev. **113**, 527 (1959).
 [7] V. F. Weisskopf, Phys. Rev. **52**, 295 (1937).
 [8] J. M. Blatt and V. F. Weisskopf, *Theoretical Nuclear Physics*

(Wiley, New York, 1952).

- [9] R. H. Fowler, *Statistical Mechanics* (Cambridge University Press, Cambridge, 1955).
 [10] H. Bethe, Rev. Mod. Phys. **9**, 69 (1937).
 [11] V. S. Stavinsky, Sov. J. Nucl. Phys. **11**, 601 (1970).
 [12] A. V. Ignatyuk, V. S. Stavinsky, and V. N. Shubin, *Nuclear Data For Reactors* (IAEA, Vienna, 1970), Vol. II.
 [13] A. V. Ignatyuk, K. K. Istekov, and G. N. Smirenkin, Sov. J. Nucl. Phys. **29**, 450 (1979).
 [14] A. V. Malyshev and Y. N. Shubin, Nucl. Phys. **76**, 232 (1966).
 [15] M. Marujama, Nucl. Phys. **A131**, 145 (1969).

- [16] G. V. Kotelnikova, G. N. Lovchikova, and O. A. Salnikov (unpublished).
- [17] J. P. Unik, J. E. Gindler, L. E. Glendenin, K. F. Flynn, A. Gorski, and R. K. Sjoblom, *Physics and Chemistry of Fission* (IAEA, Vienna, 1974), Vol. II.
- [18] C. Signarbieux, R. Babinet, H. Nifenecker, and J. Poitou, *Physics and Chemistry of Fission* (IAEA, Vienna, 1974), Vol. II.
- [19] H. R. Bowman, J. C. D. Milton, S. G. Thomson, and W. J. Swiatecki, *Phys. Rev.* **129**, 2133 (1963).
- [20] A. C. Whall, R. L. Ferguson, D. E. Troutner, and K. Wolfson, *Phys. Rev.* **126**, 926 (1960).
- [21] H. N. Erten, O. Birgul, and N. K. Aras, *J. Inorg. Nucl. Chem.* **41**, 149 (1979).
- [22] H. Naik, S. P. Dange, R. J. Singh, and S. B. Manohar, *Nucl. Phys.* **A612**, 143 (1997).
- [23] G. T. Garvey, W. J. Gerace, R. L. Jaffe, and L. Talmi, *Rev. Mod. Phys.* **41**, 31 (1969).
- [24] I. S. Gradshteyn and I. M. Ryzhik, *Tables of Integrals, Series and Products* (Nauka, Moscow, 1963).
- [25] H. M. Ahmadov and V. S. Stavinsky, *Sov. J. Prob. Atom. Sci. Tech.* **2(33)**, 36 (1979).
- [26] V. M. Piksaykin, P. P. D'yachenko, G. V. Anikin, E. A. Seregina, H. M. Ahmadov, and V. S. Stavinsky, *Sov. J. Nucl. Phys.* **28**, 313 (1978).